Atmospheric
Chemistry
and Physics
Discussions

Open Access

ACPD

Interactive
comment

Interactive comment on "Simulation of convective moistening of extratropical lower stratosphere using a numerical weather prediction model" *by* Zhipeng Qu et al.

Zhipeng Qu et al.

zhipeng.qu2@canada.ca

Received and published: 18 December 2019

1. It would be helpful if the authors would provide some information about the simu-
lated microphysical properties of the convective tops extending into the stratosphere.
Specifically, quantitative information about the simulated ice concentrations and size
distributions would be helpful. I realize the simulations use bulk parameterizations, but
the two-moment scheme should provide ice concentrations and some measure of the
width of the assumed size distribution. Realistic treatment of ice microphysics is im-
portant because the simulated convective hydration depends in part on the ice crystal
size-dependent sedimentation and sublimation of ice in the lower stratosphere.

The microphysics scheme used here predicts the ice water content (IWC) and the number concentration for 4 solid hydrometeors: ice, snow, graupel and hail. The particle size of solid categories is assumed to be gamma distribution. For the detailed parameters used in the distribution please refer to Milbrandt et al. (2005a, 2005b). Here, in order to present the results in a succinct way, we calculated the effective radius (the ratio of the third to the second moment of a droplet size distribution) for each solid category predicted by the 1.0 km simulation and weighted them with the mass. The 2D histogram of this mass weighted effective radius is shown in Fig. 1 for 19:46 UTC, 25 Aug (the same time as for Fig. 4 in the manuscript), at the altitude of ~15.5 km in domain A. At the other altitudes between 15 and 16, we find similar distributions (not shown).

The cloud overshooting tops often contain high ice water content, e.g. IWC>0.5 g m-3. In Fig. 1, we find that these air parcels containing high IWC are very few (light blue region circled). The mass weighted effective radius is between ~300 to ~700 microns which suggests that there are large particles and they will fall faster. On the other hand, for the thin ice clouds, e.g. the ice plumes, with IWC<0.1 g m-3, they occupy a much larger area comparing to the overshooting tops as they are more frequently encountered (red color). The effective radius of these solid particles is small, mostly less than 30 microns as shown in Fig. 1.

For our current study, we don't have direct observation data of ice number concentration and ice water content during the convection time. Therefore, it will be difficult to validate the results of GEM. We considered this an interesting subject for a further study, e.g. to use other aircraft in situ observations for a different case for which we have good measurements near the convection. We add in the manuscript these descriptions:

"The cloud ice properties are different in the overshooting tops and in the thin ice plumes. At the altitude of ~15.5 km (~ 1 km above the tropopause) within domain A at 19:42 UTC 25 Aug, the ice water content in the overshooting tops is relatively

high with values from ∼0.5 g m-3 up to ∼2.8 g m-3. In the thin ice plumes the ice water content is generally lower than 0.1 g m-3. We calculated the effective radius for each solid category, e.g. ice crystals, rain, snow, graupel and hail. We find that in the cloud overshooting tops, the mass weighted effective radius for ice increases with the ice water content from ∼300 to ∼700 microns. On the other hand, the mass weighted effective radius for thin ice plume is usually lower than 30 microns. The area of cloud overshooting top occupies only 2.3% of the cloudy area but contains 68% of the total ice mass at this altitude."

2. Page 1, line 30: The authors cite Anderson et al. (2012) here for the influence of water vapor on stratospheric chemistry. I believe earlier references such as Solomon et al. (1986) would be more appropriate.

Done.

3. Page 2, lines 26–30: I would recommend citing Smith et al. (2017) here.

Done.

4. Page 3, lines 17–19: It is my understanding that global models generally do not include overshooting convection. If the authors are aware of whether (or how) global models treat overshooting convection, it would be helpful to provide some discussion here.

Many GCM and global NWP models employ the mass flux approach to represent deep convection. In this approach, the updraft characteristics are calculated using a steady state plume model. This includes solving an equation for the updraft vertical velocity as a function of the evolving buoyancy of the entraining plume. The cloud top will be defined as where the vertical velocity approaches zero. This level is always above the level of neutral buoyancy. Therefore, these schemes do represent in a very simplified manner overshooting convection. How high this convection reaches depends on the environmental characteristics as well as on many parameters of the convection

scheme, namely on how entrainement and detrainment is calculated. Other complex phenomena near the tropopause during the convection are not parameterized, e.g. the falling of cloud overshooting tops, gravity wave breaking and formation of jumping cirrus, as well as the trapping of ice within the supersaturated cloud overshooting tops which inhibits ice sublimation. We will discuss all these points in details in the later parts of the manuscript. They warrant also further investigations and eventually improvements of the way of parameterizing deep convection near the tropopause. We add in this paragraph a brief discussion:

"In the global NWP and GCM models, the deep convection is parameterized using mass flux approach. The complex phenomena near the tropopause during the convection are parameterized in a simplified manner, e.g. overshooting convection, or not parameterized, e.g. the falling of cloud overshooting tops (not sedimentation), gravity wave breaking and formation of jumping cirrus, etc."

5. As shown by previous cloud-resolving model studies (e.g. Dauhut et al., 2018) the magnitude of irreversible hydration in the lower stratosphere increases as the maximum heights of overshoots extending into the stratosphere increase. It would be helpful for the authors to discuss this issue within the context of the current simulations. In addition, it would be useful to see how the distribution of overshoot maximum heights depends on the model spatial resolution.

For the fully solved high resolution simulations, the maximum height of the cloud overshooting top depends on the model horizontal resolution. In our simulated case, the maximum heights are 16.64 and 16.96 km for 2.5 and 1.0 km simulation. For 0.25 km simulation, the early stage of the convection was simulated in the limited green box in Fig. 1 with a maximum height of 16.64 km. The irregularity here is probably due to the lack of the latter period of the convection for the 0.25 km simulation (in the other simulations, the maximum heights are often found in the later period). Nevertheless, we can conclude that the higher the model horizontal resolution is, the higher the cloud overshooting top will reach in the lower stratosphere. As for the 10 km simulation with

parameterized convective cloud, as mentioned in the previous question, the height of cloud overshooting top depends on the environmental characteristics as well as on many parameters of the convection scheme, namely on how entrainement and detrainment is calculated. It will not be reasonable to compare directly the 10 km simulation with the other high resolution simulations, even though the maximal cloud top height of 10 km simulation (16.13 km) is lower than all the other high resolution simulations. We modified the manuscript and discussed this point later in the manuscript:

"It is not a surprise that the higher resolution NWP models tend to produce stronger direct vertical transports across the tropopause because, as shown in Subsection 3.1, the transport is closely related to the strength of overshooting and the breaking of the gravity waves. Similar to what was found by Weisman et al. (1997), we find in our GEM simulations that the simulated maximal vertical wind speed is inversely proportional to the horizontal grid-spacing of the NWP model. The stronger vertical wind speed in the convection updraft leads to higher cloud overshooting top. In our cases with high resolution simulation, the maximum cloud top altitude is 16.64 and 16.96 km for 2.5 and 1.0 km simulation respectively. We find that the stronger overshooting wind speed in the higher resolution simulations leads to favorable conditions for gravity wave breaking (see the discussions in Subsection 3.1) and thus more direct vertical transport. This agrees with Dauhut et al. (2018). In total, the direct vertical transport of water vapor contributes to 40% of the total transport at the tropopause level for the 2.5 km simulation and makes up to 89% for the 1.0 km simulation."

6. Page 4, line 29: It is confusing (and possibly misleading) to refer to the aircraft flight paths as "trajectories". It would be better to use terminology such as "flight path" or "aircraft altitude profile".

Done.

7. Page 5, lines 1–10: Smith et al. (2017) also did a trajectory analysis to determine the convective systems responsible for the observed lower-stratospheric water vapor

plumes. It would be helpful if the authors compared the results/conclusions from the trajectory analysis done here with Smith et al. (2017).

Smith et al. (2017) focused on the high water vapor content observed by the ER-2 aircraft between ~19:30 to ~19:50 UTC (the third dive in Fig. 2 of the manuscript) in the north-most part of domain B at the level near ~100 hPa. The source of the humid air parcels observed there are mostly traced back to the convection east to the Lake Superior between 26 Aug 2013 21:00 UTC and 27 Aug 2013 12:00 UTC (hereinafter named convection Day2). Our back trajectory calculation gives similar results as shown for a humid air parcel from the northeast of domain B (Fig. 2 in this response, dashed back tracking line) which is traced back to the area of convection Day2. We note that the simulated convection initiated at the end of 26 Aug is slightly north to the real convection observed by satellite image (a location error in the simulated convection). This justifies the use of average of domain B, as opposed to individual location(s), for the evaluation so that humid areas linked to the convection Day2 are always included.

One of the foci of current paper is the average of water vapor content profile in the domain B. As explained above, this is designed to tolerate the spatial-temporal errors of the model simulations. For the southwest of domain B, the humid air parcels are mostly traced back to the convection that happened east to the Lake Superior between 25 Aug 17:40 UTC and 26 Aug 05:40 UTC (hereinafter named convection Day1). This is shown in Fig. 2 by the solid red back trajectory line. Having inspected these trajectory results, we found that the contribution for the average water vapor content in domain B by the convection Day1 (southwest) is more important than that of the convection Day2 (northeast). We therefore focused more on the convection Day1 in most parts of the manuscript, e.g. the convection shown in Fig. 3 of the manuscript as well as the budget analysis in section 3.4.

We added in the manuscript a brief discussion for the comparison with the results of Smith et al. (2017):

"Using this technique, we find that the large water vapor anomalies observed by the aircraft in Domain B on 27 Aug 2013 originated from two deep convection events. The first one began at the end of 25 Aug and ended at the beginning of 26 Aug in Domain A (100ËŽ W to 87.5ËŽ W, 46ËŽ N to 50ËŽ N, ∼860x445 km2) as illustrated in Fig. 1 (see more discussions below). This convection has major contribution to the water vapor content in the lower stratosphere of domain B. The second source is the convection began at the end of 26 Aug and ended at the beginning of 27 Aug in Domain A. This second convection increases the water vapor content in the northern part of domain A. This agrees with the results of Smith et al. (2017) in which the humid air parcels observed by the aircraft near 19:40 UTC (Fig. 1, northeast of domain B) are traced back to the convection began at the end of 26 Aug."

8. Figure 4 is presumably a longitude slice through Domain A. An x-axis should be provided. Also, does this slice correspond to a particular latitude, or are the authors averaging over latitude within Domain A?

The cross-section presented in Figure 4 of the manuscript is not along a longitude but along a skew line. We added a separated panel (e) in Figure 4 of the manuscript to show the location of this cross-section within the domain A.

9. Page 8, line 24: The authors discuss the simulated moisture enhancement in the lower stratosphere. How is this enhancement calculated? Is a difference taken between the post-convection moisture field and the pre-convection field?

Thanks, it's a good question. The profiles shown in Fig. 6a in the manuscript is for the average water vapor mixing ration during the 5 hours' evaluation time within domain A. The horizontal transport of water vapor should therefore have an impact on those profiles. In a more direct way, by comparing the averaged profiles before and after the convection in Fig. 3, we can see an enhancement of water vapor mixing ratio above the altitude of 16 km, but not between 15 and 16 km for the two high resolution simulations. This is mostly due to the horizontal transport of water vapor out of domain A through the

western and southern borders. For the altitude between 15 and 16 km, the horizontal wind speed is fairly high (Fig. 5e of the manuscript). Therefore, the impact on the comparison of vertical profile is significant. On Fig. 4a, the water vapor mixing ratio field on the level of $\sim$15.5 km is shown. At this time the convection just began. We find humid air in majority part of the domain A, except the westmost part. These humid areas are linked to the convection happened during the previous day (24 Aug). During the evaluation period on 25 Aug, the convection we focused on injected a large amount of water vapor into this altitude. Meanwhile, most of the humid air presented at the beginning of the evaluation time is moving out of the domain. This caused eventually a decrease of the average humidity within domain A as shown in Fig. 3a.

After rethinking about the statement here about the enhancement of water vapor, we considered that it is not suitable to mention it here because the conclusion could not be derived directly form Fig. 6a of the manuscript. A better way to evaluate the enhancement of water vapor is to calculate how much water vapor is transported vertically through the tropopause. This calculation is discussed in detail in the later section of the manuscript (section 3.4, budget analysis).

The main purpose of Fig. 6a (manuscript) is to show that 10 km simulation produce clearly moister lower stratosphere than the two high resolution simulations. We modified the text as follow:

"We further examine the water vapor fields simulated by GEM at different horizontal grid-spacings. Fig. 6a and 6b show the mean vertical profiles of water vapor volume mixing ratio and temperature within the afore-defined Domain A and 5-hour time window. All the simulations show irregular moisture profiles near 16 km, where the vertical trend of the humidity profiles bends and produces 'bumps' (elevated water vapor contents) above the tropopause (indicated by the circles in Fig. 6, hereinafter the tropopause is defined by the altitude where the mean lapse rate Γ within Domain A and 5-hour time window decreased to 2ËŽC km-1 or less)."

10. Page 9, lines 5–10: The authors discuss errors, uncertainties, and biases in the MLS H2O retrieval. However, my understanding is that the 100-hPa retrievals that are most relevant for this paper are in good agreement with observations.

Agreed. In response to the comments of the other reviewer, we updated the way of comparison between MLS data and GEM data by applying the averaging kernel of MLS to GEM profiles. This allows a more coherent comparison as suggested by another referee. The results are shown in the updated Fig. 6c, 6d of the manuscript (or the Fig. 5c and 5d of the response). For the pressure levels near 100 hPa, we observed moister air from both GEM simulations which might indicate the overestimation of water vapor from the model simulation. The 10 km simulation gives even higher water vapor mixing ratio than the 2.5 km simulation and MLS, which evidences the positive bias in the low resolution model. On the other hand, near the levels of 160 hPa, we can see significant differences between the model simulations and the MLS retrievals. At these lower levels, the MLS data might subject to the negative bias reported by Hegglin et al. (2013), Vömel et al. (2007) and Livesey et al. (2018). This makes the comparison more uncertain; hence the validation against aircraft data is used.

We modified the text in the manuscript concerning the comparison between model simulations and MLS data:

"Figure 6c, 6d show the comparisons between the GEM simulations after applying averaging kernels of MLS and MLS retrievals (v4.2). Because of the scarcity of the collocated satellite data and also the afore-mentioned mismatch in time and location of the simulated convective system, we conduct the comparison with respect to area-averages rather than individual samples. The MLS measurements used here include five MLS footprints located between [38 N, 45 N] and [95 W 93 W], taken on 26 Aug 2013 around 19:00 UTC, about 15 hours after the dissipation of the convection system (Fig. 7, red diamonds). We applied the averaging kernel of MLS on the mean profiles of GEM simulated humidity and temperature within the 100x100 km regions centered on the MLS footprints. The comparison here suggests that both model simulations give

higher estimations of water vapor content in the UTLS comparing to MLS retrievals, although the higher-resolution simulation better approximates the satellite observations. It is also found that GEM slightly overestimated the temperature comparing to MLS retrievals. This suggests that warmer temperatures in comparison to MLS could lead to slower ice crystal growth and thus less dehydration and thus higher gas-phase water. The spatial-temporal errors of the model simulation, e.g. shifted convection location or time, might also contribute to the discrepancies between the GEM and MLS profiles. Furthermore, the lower value of water vapor content from MLS near the level of 160 hPa may be subject to the aforementioned negative bias in the MLS data."

11. Section 3.4: I believe this section could be better organized. There seems to be a fair amount of repetition, and the discussion seemed to meander. Perhaps this section could be more concise, and a sentence or two at the beginning outlining the analysis techniques would be helpful.

Some changes of the structure are made. Please refer to the modified manuscript for details.

Interactive comment on Atmos. Chem. Phys. Discuss., https://doi.org/10.5194/acp-2019-823, 2019.
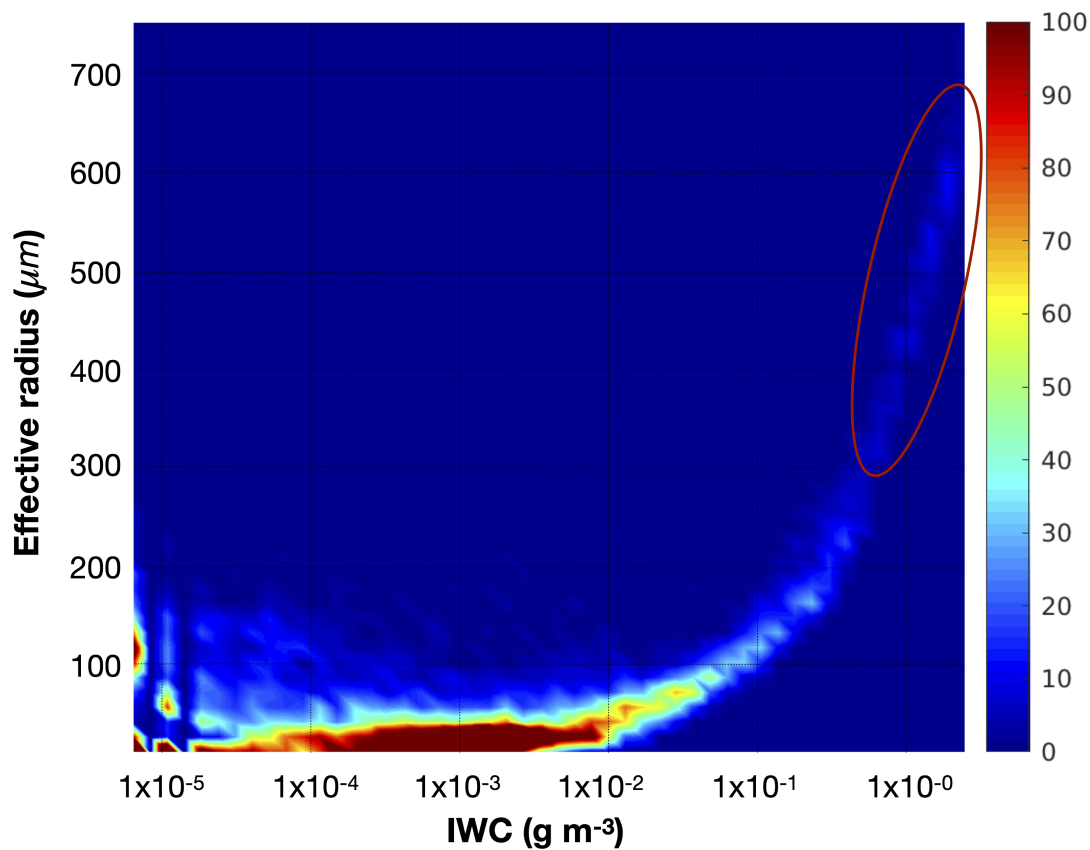
Fig. 1. 2D histogram of cloud ice in domain A at the altitude of 15.5 km, 19:46 UTC 25 Aug. x-axis: ice water content; y-axis mass weighted effective radius. 50 bins are used in each axis.

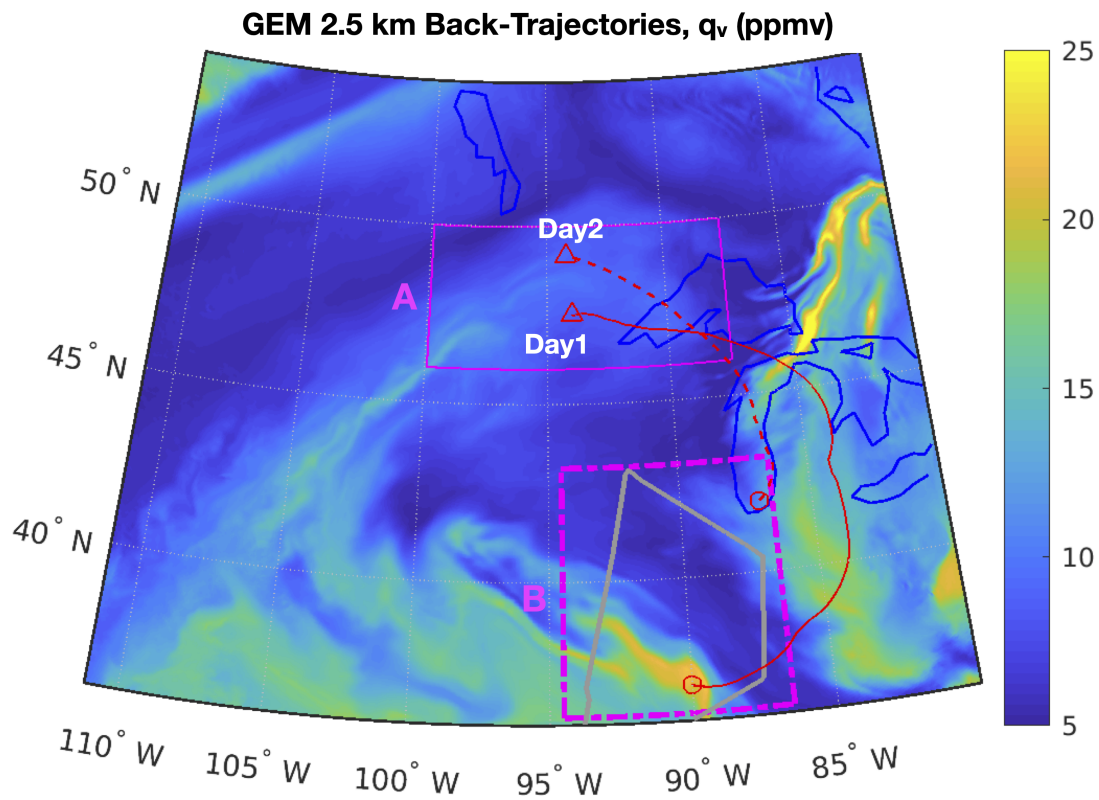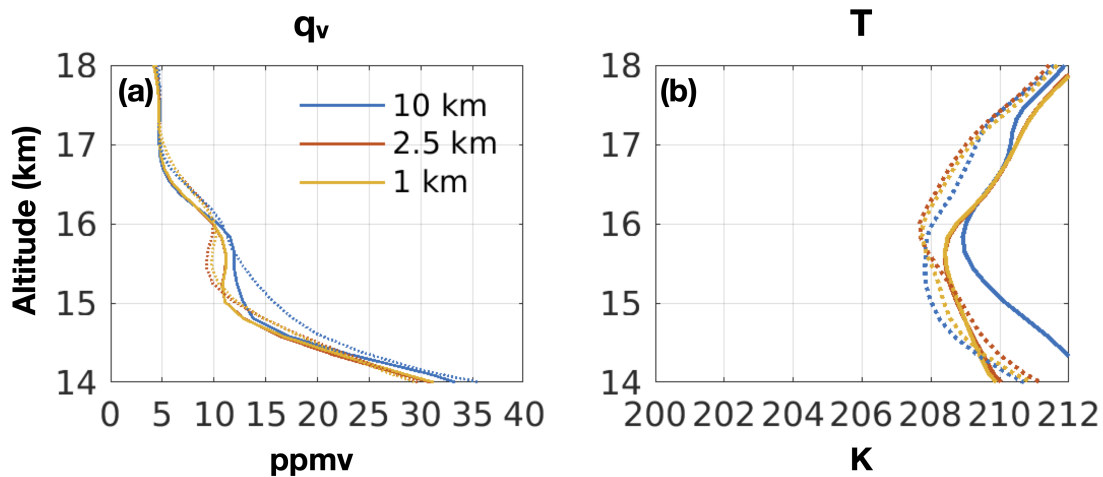**Fig. 2.** Back tracking from 19:40 UTC 27 Aug to: 22:40 UTC, 25 Aug for convection Day1, and to 21:00 UTC 26 Aug for convection Day2.

Fig. 3. The mean profiles of water vapor volume mixing ratio (qv) and temperature (T) for Domain A before (solid lines for 18:00 UTC, 25 Aug) and after (dotted lines for 23:00 UTC, 25 Aug) the convection.
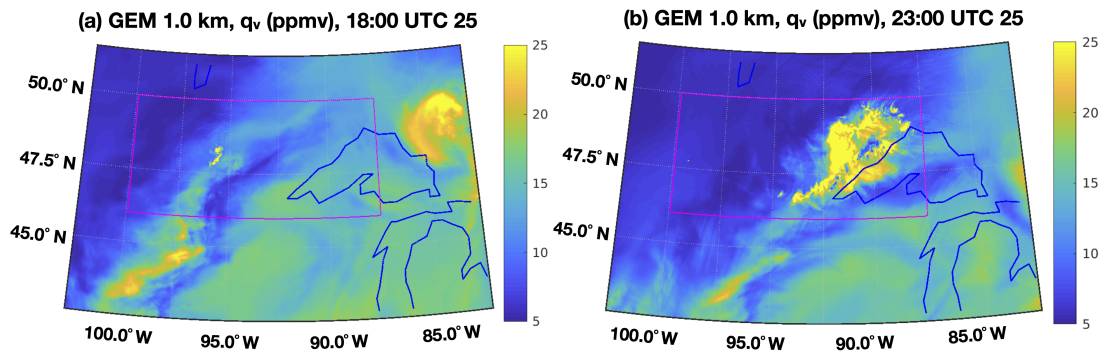
Fig. 4. The water vapor mixing ratio field at the altitude of ~15.5 km before (a) and after (b) the convection on the day of 25 Aug. The magenta box represents the domain A.
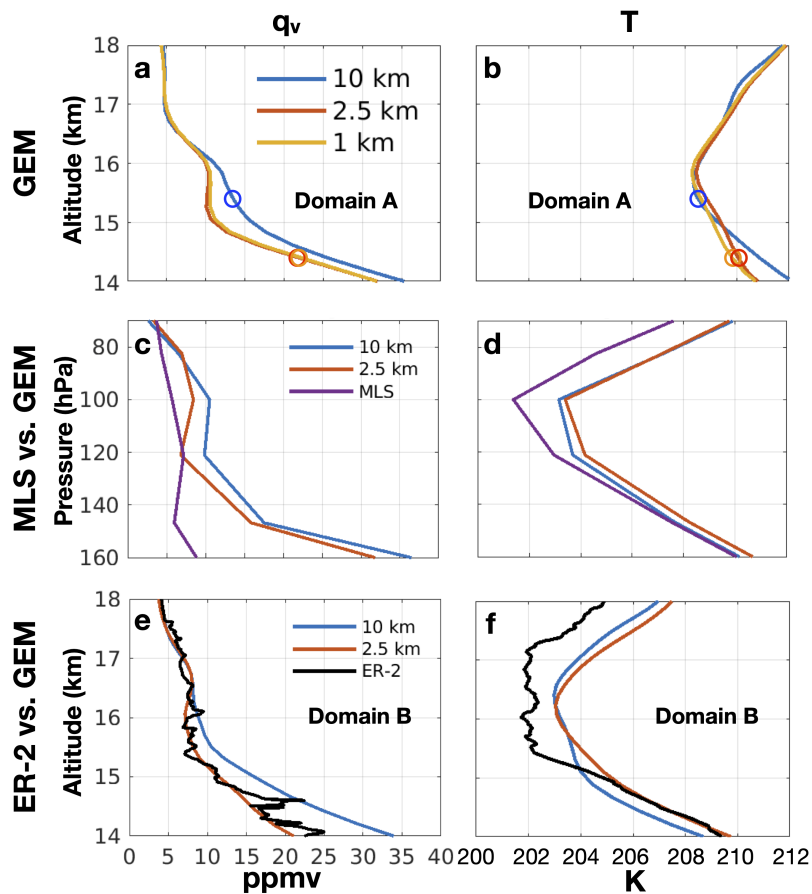
Fig. 5. Same to Figure 6 in the manuscript, except c), d) mean profiles (qv and T) after applying averaging kernels of MLS on GEM 2.5 km, 10 km simulation.